REVIEW

Designing Membrane Electrode Assembly for Electrochemical CO$_2$ Reduction: a Review

Xuerong Wang[1] · Shulin Zhao[1] · Tao Guo[1,2] · Luyao Yang[1] · Qianqian Zhao[1] · Yuping Wu[1] · Yuhui Chen[1]

Abstract

Currently, the electrochemical CO$_2$ reduction reaction (CO$_2$RR) can realize the resource conversion of CO$_2$, which is a promising approach to carbon resource use. Important advancements have been made in exploring the CO$_2$RR performance and mechanism because of the rational design of electrolyzer systems, such as H-cells, flow cells, and catalysts. Considering the future development direction of this technology and large-scale application needs, membrane electrode assembly (MEA) systems can improve energy use efficiency and achieve large-scale CO$_2$ conversion, which is considered the most promising technology for industrial applications. This review will concentrate on the research progress and present situation of the MEA component structure. This paper begins with the composition and construction of a gas diffusion electrode. Then, the application of ion-exchange membranes in MEA is introduced. Furthermore, the effects of pH and the anion and cation of the anolyte on MEA performance are explored. Additionally, we present the anode reaction type in MEA. Finally, the challenges in this field are summarized, and upcoming trends are projected. This review should offer researchers a clearer picture of MEA systems and provide important, timely, and valuable insights into rational electrolyzer design to facilitate further development of CO$_2$ electrochemical reduction.

Graphical Abstract
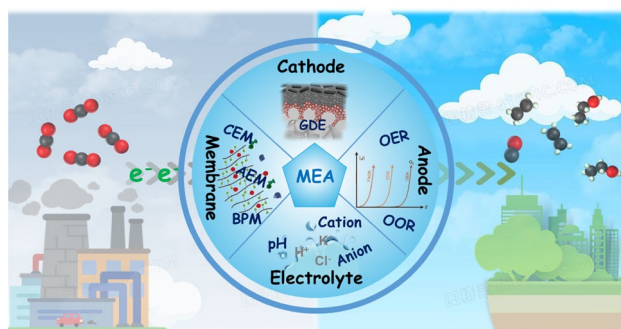
Xuerong Wang and Shulin Zhao have contributed equally to this work.

✉ Yuhui Chen
cheny@njtech.edu.cn

1 State Key Laboratory of Materials-Oriented Chemical Engineering, and School of Energy Science and Engineering, Nanjing Tech University, Nanjing 211816, China

2 Jiangsu Academy of Environmental Industry and Technology Corp, Nanjing 210036, China

Introduction

The energy shortage and environmental deterioration caused by reckless fossil energy consumption have become the most important global problems faced by mankind. Using renewable energy sources like solar and wind power could effectively address energy and environmental issues in the future [1, 2]. To ensure the continuity and stability of renewable energy generation and power supply, new energy

storage technologies must be developed and utilized. Using renewable electricity to drive the conversion of CO_2 has attracted much attention because it not only effectively solves the mismatch between electricity supply and demand but also enables the conversion of CO_2 into value-added carbon-based products (e.g., carbon monoxide, formic acid, methanol, ethylene, and propanol) [3, 4]. As an effective way to achieve clean and low-carbon energy transformation, the CO_2 reduction reaction (CO_2RR) technology anticipates that the reliance on conventional fossil fuels for energy demand will be eliminated. Although electrocatalytic CO_2RR has shown promising prospects and application potential, the development of this technology remains incipient and faces many obstacles, including high overpotential, low current density, unsatisfactory product selectivity, hydrogen evolution reaction (HER) competition, and poor stability. To surmount these obstacles, many attempts have been made to develop efficient catalysts and improve electrolytic devices [5, 6].

Recently, most of the strategies to enhance CO_2RR performance have focused on regulating electrocatalysts, which has remarkably expanded the knowledge and understanding of CO_2RR [7–9]. However, this knowledge remains far from being used in industrial settings, particularly in terms of current density [10]. It is common knowledge that the overall performance of the CO_2RR system is directly influenced by various components, such as electrocatalysts, electrolytes, ion-exchange membranes, and electrolytic cells, which form a comprehensive electrochemical CO_2RR system. Therefore, an economically feasible CO_2 reactor must be rationally designed. At the present stage, most studies are conducted on the basis of H-cells, which are easy to assemble, simple to operate, low in cost, reflect the intrinsic activity of catalysts directly, and are suitable for swift assessment and screening of electrocatalytic materials (Fig. 1a). Nevertheless, the limited capacity for CO_2 dissolution (< 0.034 mol/L) and poor mass transport pose challenges in achieving the desired current density for industrial implementation (200 mA/cm^2) [11]. Therefore, the exploration of flow cells has developed and spread gradually.

At present, the CO_2RR flow cell mainly includes a three-compartment microfluidic cell and a membrane electrode assembly (MEA) reactor (Fig. 1b–e). The microfluidic cell
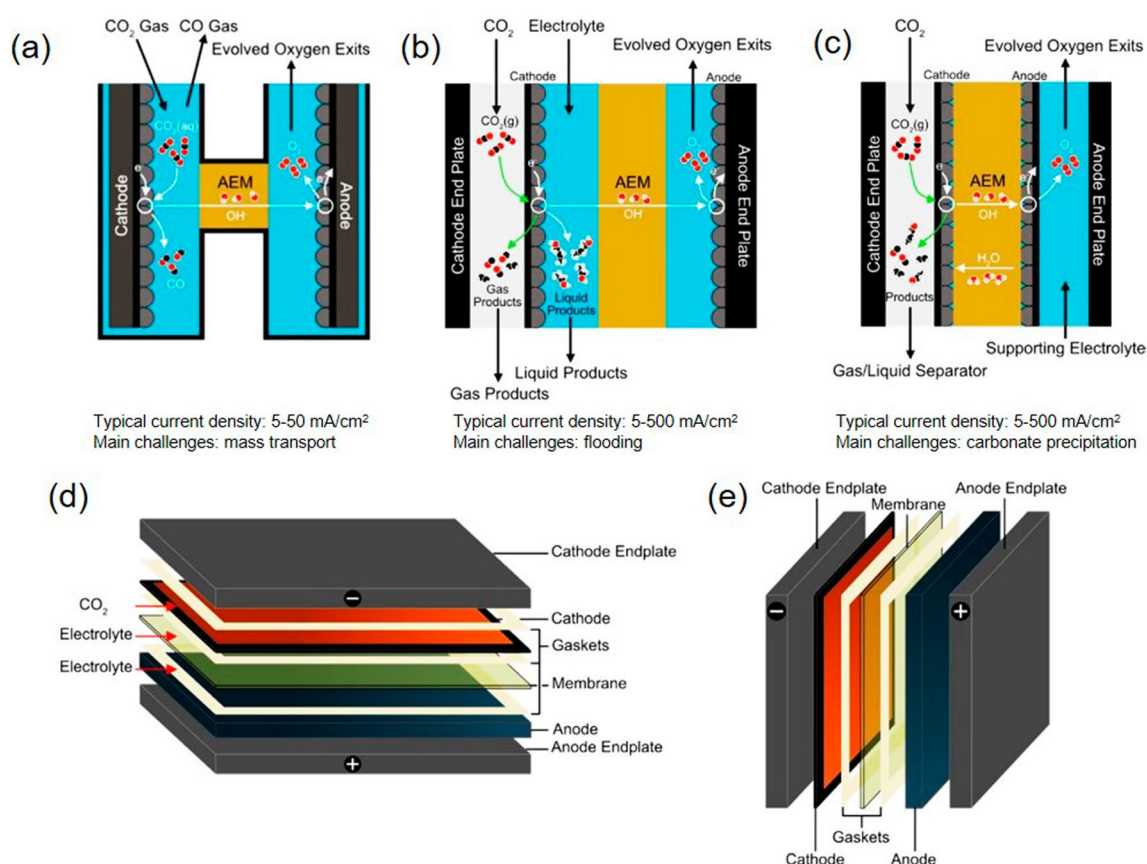

Fig. 1 Schematic of common CO_2 electrolyzers. **a** Typical H-cell electrolyzer. **b** Three-compartment microfluidic electrolyzer. **c** MEA electrolyzer. Illustrations of **d** a three-compartment electrolyzer and **e** a MEA electrolyzer. An anion exchange membrane (AEM) is selected as a membrane example. Reproduced with permission from Ref. [12]. Copyright 2022, American Chemical Society

comprises three flow channels utilized for transferring the CO_2 gas cathode electrolyte and anode electrolyte, respectively (Fig. 1b, d). To separate the catholyte from the channels containing CO_2 gas, a gas diffusion electrode (GDE) is employed. The catalyst layer (CL) is deposited on the side in contact with the electrolyte, and CO_2 is transported to the catalyst through the back of the GDE. The design of microfluidic cells effectively addresses the issue of CO_2 dissolution and restricts diffusion in conventional H-type cells, substantially enhancing the reaction current. In addition, this design can be used with high-concentration alkaline electrolytes (such as KOH), which not only hinders the competition from the HER but also lowers the energy barrier for the CO_2RR, thus improving the reaction selectivity. However, many problems remain to be addressed, including issues such as electrolyte flooding and salt precipitation. The main difference between MEA and microfluidic cells lies in the use of a cathode electrolyte (Fig. 1c, e) [12]. For MEA, the catholyte-free design lowers the Ohmic loss and, to a certain extent, solves the problems of electrolyte flooding, the deposition of electrolyte impurities on the catalyst surface, and carbonate crystallization, which contributes to improving the stability of the entire system. Currently, enthusiasm for developing MEA is considerable because of its enhanced energy use.

Herein, we initially discussed the MEA configuration, including the GDE and ion-exchange membrane, and subsequently summarized the impact of pH and the anion and cation of the anolyte on MEA performance. Next, we analyze the CO_2RR-coupled anodic reactions. Finally, this paper delves into the challenges faced by MEA and outlines its prospective avenues for future development.

This review aims to serve the practical application of MEA and understand the reaction mechanism.

Characteristics and Functions of the Core Components of a MEA Electrolyzer

Engineering the Cathode GDE

The GDE is the core part of a MEA, the place for electrochemical reactions. It promotes the diffusion of CO_2 to the catalyst surface by providing a porous and hydrophobic transport channel. The use of a GDE can increase the current density of the CO_2RR by one to two orders of magnitude (> 1 A/cm²) [13]. Increasingly, more research works have found that designing and preparing different GDEs to regulate the interface is a key technology for affecting CO_2RR performance [14, 15]. Many excellent GDEs have been designed for use in flow cells [14, 16]. However, the optimization of GDEs for a flow cell may not be easily applicable to a MEA because of their distinct structural differences. Therefore, the composition of the GDE in an MEA must be understood to optimize its performance in the MEA. Generally, the basic GDE structure comprises a gas diffusion layer (GDL), a current collector (CC), and a CL (Fig. 2) [17]. A satisfactory combination of these three components helps realize the stable running of the entire reaction process. Among these components, the GDL not only provides an abundant CO_2 transport channel but also supports the CL to ensure a high electrolyte diffusion rate. The CC is mainly used to maintain satisfactory electronic transmission efficiency of the system to minimize resistance loss throughout the device. CL is the most crucial part of

Fig. 2 Schematic of a gas diffusion electrode (GDE)
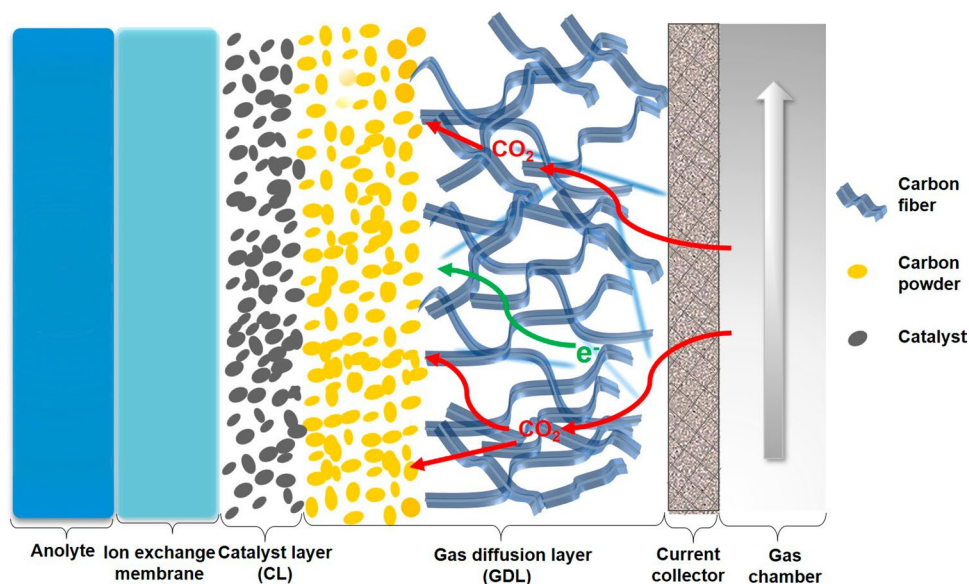
CO_2RR because it directly affects product purity, production, and configuration.

To fabricate a GDL, the first step is to select a suitable macroporous substrate (MPS). Hydrophobically treated carbon-based matrices featuring haphazardly linked carbon fibers are frequently the material of choice for MPS because they offer a stable and flexible support structure. The average pore size of carbon fibers is 20–100 μm, which provides a desirable channel for gas transport and electron transfer [18]. After the MPS is determined, the next step is to build the microporous layer (MPL). This layer comprises carbon powder and a hydrophobic agent, amalgamating the MPS and CL. To generate porous channels, the traditional method of producing an MPL involves repeatedly spraying and heating a precursor ink comprising carbon powder and a hydrophobic agent [18]. The suitable hydrophobicity of MPS and MPL aids in creating an abundant three-phase interface between the reactant and the catalyst [19, 20]. Currently, a commonly used hydrophobic agent is polytetrafluoroethylene (PTFE) [21]. Velayutham et al. [22] investigated the impact of PTFE concentration in MPS and MPL on the performance of a polymer electrolyte membrane fuel cell. In the MPS and MPL, the ideal content of PTFE was determined to be 23 wt% and 20 wt%, respectively, which was further

validated in the CO_2RR. Kim et al. [23] examined the effect of varying the PTFE mass fraction in the MPL (4.5–50%) on the electroreduction activity of CO_2 and proposed that the optimal mass fraction of PTFE was 20%. In this scenario, CO_2 reduction exhibits the least charge transfer resistance, resulting in the highest conversion current density of the CO product, reaching a value of 280 mA/cm² (Fig. 3a–c). Further, Weng et al. [17] established the relationship between the hydrophilicity of the GDL and current density based on a multiphysics model and proposed that under the condition of high current density (> 100 mA/cm²), if the GDL is too hydrophilic, the cathode will suffer from flooding, which will affect the distribution of CO_2 in the CL. If the current density of CO_2 conversion is further increased, the catalyst load should be lowered accordingly. To overcome flooding damage to equipment stability, Zhong et al. [24] fabricated a sandwich structure, polyethylene-PTFE/catalysts/carbon nanoparticles, so that the densely layered PTFE offers strong hydrophobicity to maintain the liquid/gas/solid interface for 100 h of electrolysis operation.

In the MPL, carbon powder also plays a vital role. The type of carbon powder, particle size, and proportion to the hydrophobic agent are crucial to the electrode's conductivity and microstructure [25]. Graphite, acetylene black, and
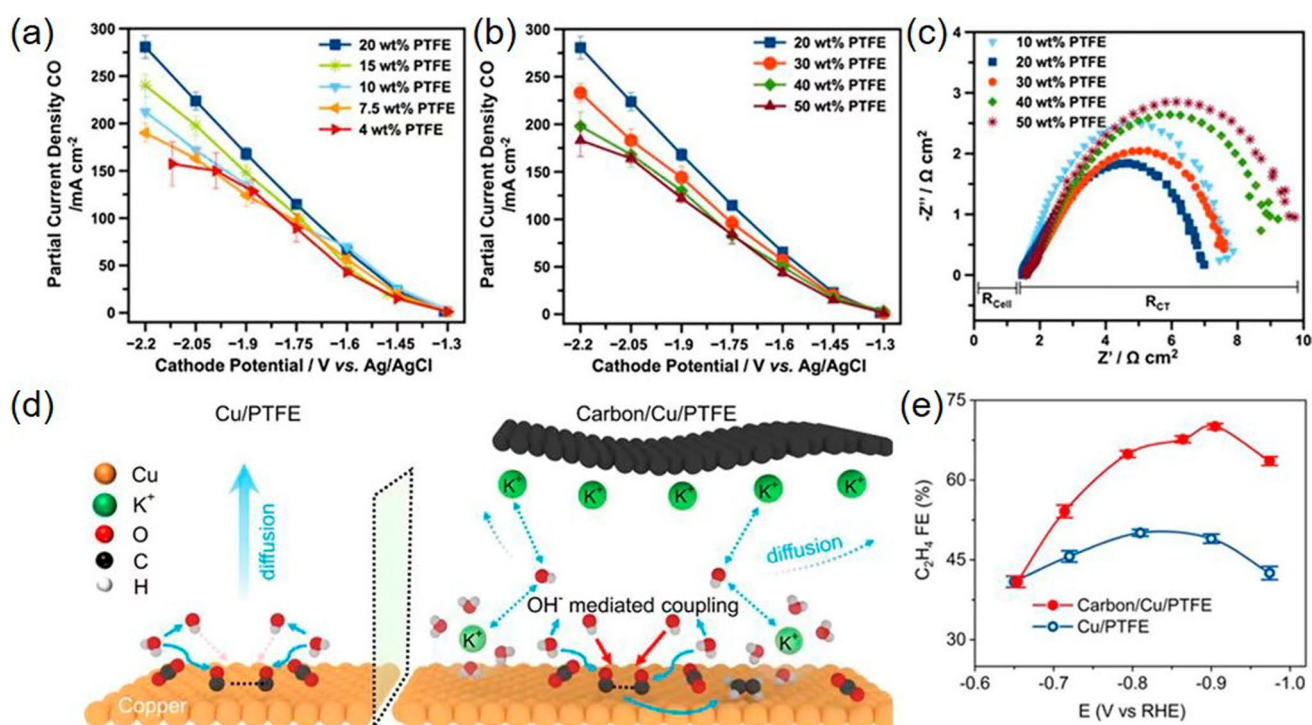

Fig. 3 Partial current density for CO varying with the potential of GDEs consisting of MPLs with different amounts of PTFE: **a** 4.5, 7.0, 10.0, 15.0, and 20 wt%; **b** 20, 30, 40, and 50 wt%. **c** Impedance spectra for GDEs at a cell potential of 2.0 V. Reproduced with permission from Ref. [23]. Copyright 2016, Elsevier. **d** Depiction of the in situ restriction impact on OH^- for the carbon layer. **e** Potential-dependent $FE_{C_2H_4}$ on carbon/Cu/PTFE and Cu/PTFE. Reproduced with permission from Ref. [26]. Copyright 2023, American Chemical Society

carbon black are commonly used carbon powders. Large particles harm CO$_2$ transport, while the GDL is easily flooded if the particles are too small, and thus, it gradually loses stability during the reaction. The ideal size range is between 5 and 20 μm. Using the abovementioned PTFE content, Orogbemi et al. [25] found that a combination of 20% PTFE and 80% carbon black yielded optimal gas penetration. Furthermore, the incorporation of carbon powder can help regulate the catalyst's environment. Wang et al. [26] suggested that the carbon layer can trap the OH$^-$ produced in situ while undergoing the CO$_2$RR procedure through electrostatic confinement, providing a localized alkaline catalytic interface in a neutral environment. The carbon layer on the Cu/PTFE electrode dramatically improved the Faraday efficiency (FE) of CO$_2$-to-ethylene in a neutral medium from 47 to 70% with a maximum $j_{ethylene}$ of 381 ± 4.94 mA/cm^2 (Fig. 3d, e) [26].

In addition, to construct GDEs, researchers often use binders, which are ionic monomers incorporated into catalyst inks, to enhance their consistency, conductivity, and adhesion to MPL surfaces. Most studies use Nafion as the binder. Interestingly, alternative binders also influence the CO$_2$RR. Liu et al. [27] compared the application of a GDE with silver nanoparticle catalyst inks prepared using two typical ionic polymer materials (Nafion and Fumion) as binders to an MEA electrolytic cell. Fumion-containing GDE can maintain very high CO selectivity for a long time, which is superior to that of Nafion-containing inks

Fig. 4 Results of the CO$_2$RR performance of Nafion- and Fumion-fixed GDEs. **a** Variation in the FE$_{CO}$ over time. **b** Temporal variation in the measured electrode potential. **c** Amount of K$^+$ passed through the electrolyzer. Reproduced with permission from Ref. [27]. Copyright 2023, Elsevier

(Fig. 4a, b). The difference in electrolytic stability was not due to the difference in hydrophobicity. The K$^+$ content in the liquid brought out of the outlet was measured, and it was found that the effective expulsion of metal cations was more important for the life of the MEA than the GDE's infiltrability (Fig. 4c), which also highlighted the superiority of Fumion as a binder.

Engineering the Ion-Exchange Membrane

The ion-exchange membrane is another core component of the MEA system and has an important impact on overall CO$_2$RR performance [28]. The ion-exchange membrane can separate the anode and cathode of an electrolytic cell, effectively preventing the oxidation of reduction products in the anode and maintaining the overall ion balance of the system. The ideal ion exchange membrane should have satisfactory ion conductivity, high mechanical strength, and sufficient chemical stability to maintain a continuous working life of thousands of hours. The type of ion-exchange membrane affects the type and rate of ion transport [29, 30]. At present, the MEA CO$_2$RR system uses three different ion-exchange membranes: an anion exchange membrane (AEM), a cation exchange membrane (CEM), and a bipolar membrane (BPM) (Fig. 5a–c) [16, 31].

An AEM selectively transfers anions (such as HCO$_3^-$ and OH$^-$) from the cathode to the anode. The use of an AEM provides protons to the cathode by utilizing the humidity in the gas stream and/or membrane as a water source [15]. Because of the reduced amount of protons available, an AEM has been employed to handle the severe HER suffered with CEM [32]. Jiang et al. [33] constructed an MEA with an AEM, an IrO$_2$ anode, and a Ni single-atom cathode. When the current density was 400 mA/cm^2, the selectivity for CO achieved a remarkable 97%. Theoretically, if only OH$^-$ ion transport occurs in the electrolyte membrane, it is helpful to maintain a relatively stable cathode reaction environment and relatively high ion conductivity. However, in the real electrode process, OH$^-$ reacts with CO$_2$, resulting in HCO$_3^-$/CO$_3^{2-}$ species formation under alkaline conditions. Figure 5d depicts the solubility of CO$_2$ based on pH. As the pH increases, the existing CO$_2$ progressively changes into HCO$_3^-$ and CO$_3^{2-}$ [34]. Therefore, the relatively low mobility of HCO$_3^-$/CO$_3^{2-}$ ions increases the Ohmic polarization loss of the MEA [35]. At the same time, for example, KHCO$_3$ can block the pores of GDE, preventing the transmission of CO$_2$ [36, 37]. In addition, HCO$_3^-$/CO$_3^{2-}$ species selectively reaching the anode through the AEM is equivalent to CO$_2$ being transferred to the anode, considerably decreasing the fuel efficiency of CO$_2$ conversion.

The CEM electrolyzers facilitate the transfer of protons or other cations from the anode to the cathode via the exchange membrane, resulting in an acidic pH on the cathode surface
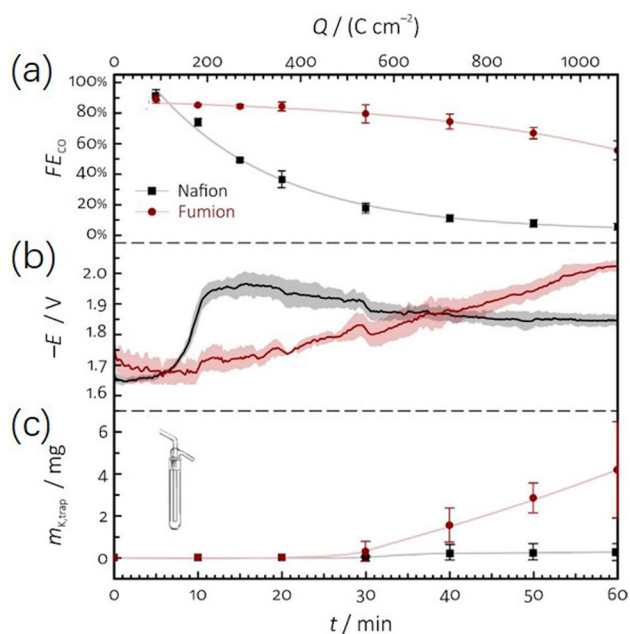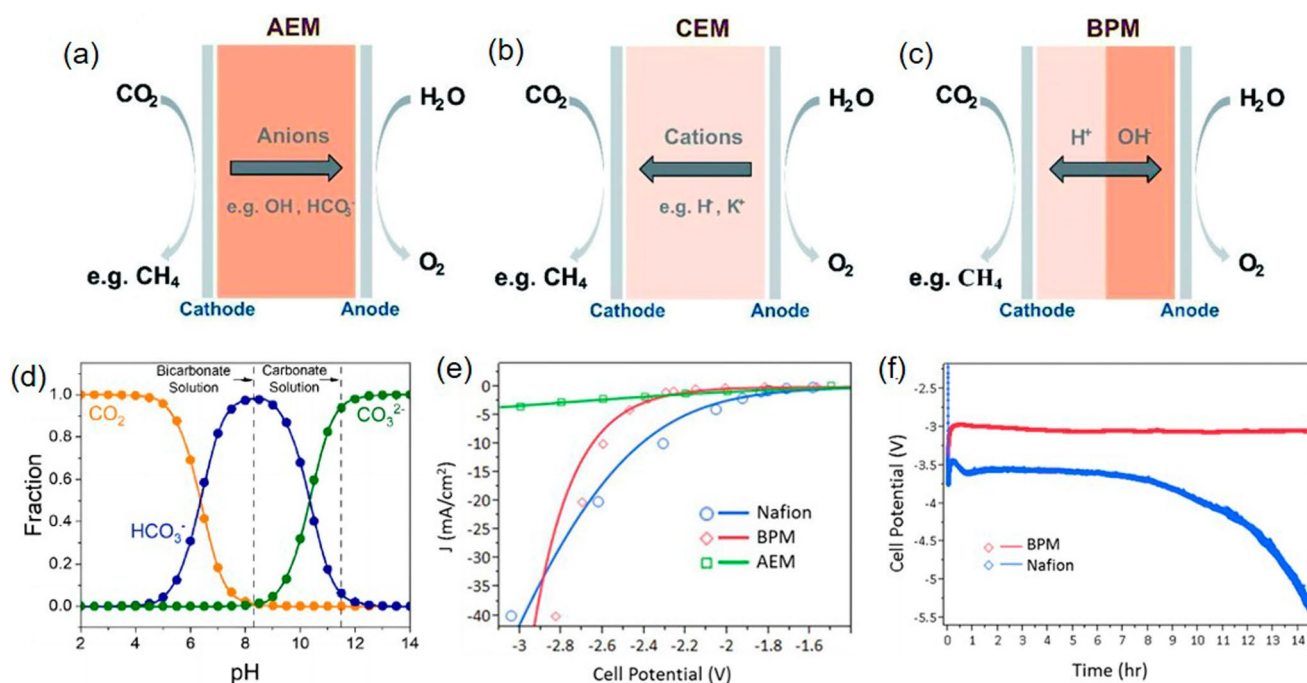
Fig. 5 Overview of ion transport pathways for the three types of ion-exchange membranes: **a** AEM, **b** CEM, and **c** BPM. Reproduced with permission from Ref. [16]. Copyright 2021, Royal Society of Chemistry. **d** Partial pH dependence of the carbonate system. Reproduced with permission from Ref. [34]. Copyright 2023, American Chemical Society. **e** *J–V* curves for the MEA system comparing bipolar, anion exchange, and Nafion membranes. **f** Comparing the stability of BPM and Nafion membranes under a current density of 80 mA/cm². Reproduced with permission from Ref. [45]. Copyright 2016, American Chemical Society

and preventing HCO_3^-/CO_3^{2-} formation at the cathode interface [38]. Nafion® membranes are typical CEMs. An MEA with a CEM has demonstrated improved performance over liquid-phase flow cells, which is related to increased CO_2 availability. Lee et al. [39] indicated that a catholyte-free electrolyzer provided sufficient dissolved CO_2 for the cathodic reaction, considerably increasing the selectivity for formate compared with a liquid-phase electrolyzer. However, acidification of the cathode will occur at a high current density in the MEA with a CEM, leading to a severe HER, which reduces the conversion efficiency of the CO_2RR [40].

Recently, a BPM has been applied in CO_2RR systems [41, 42]. The BPM promotes water dissociation to generate OH^- and H^+, which are then transported to the anode and cathode, respectively. The problem of voltage fluctuation and instability caused by a pH gradient in the monopole membrane system is resolved using the BPM and ensuring consistent pH levels at the anode and cathode [43, 44]. Li et al. [45] constructed an MEA configuration with a BiO_x gas diffusion cathode and a $NiFeO_x$ anode in which a BPM was used for the first time. The BPM exhibits a lower electrical resistance than the AEM or Nafion® membrane. The BPM-MEA cell voltage can be stabilized at 3.0 V for 14 h at 80 mA/cm², and the CO FE is nearly 60%. If the Nafion® membrane is used as a membrane, MEA will be deactivated

after 7 h because of anodic OH^- depletion (Fig. 5e, f). It is seen that the ion transport mechanism of the BPM helps inhibit the change in cathode pH. Yang and coworkers [46] constructed an MEA system coupled with a BPM, which reduced CO_2 loss by five times compared with the AEM. The FE_{CO} increased from less than 20% to 68%. The H^+ generated by the membrane electrode effectively inhibited the loss of CO_2. However, Vermaas et al. [47] noted that when the pH difference between the anode and cathode is minuscule, the energy consumption required to drive the hydrolysis in a BPM is relatively high, considerably reducing the energy efficiency for CO_2 conversion.

In summary, maintaining effective CO_2 mass transfer and the local reaction environment for a catalyst is crucial for improving the CO_2RR performance of an MEA system. At present, the material design and overall performance of ion-exchange membranes still have considerable room for improvement.

Electrolyte Effects in MEA Electrolyzers

Because an MEA electrolyzer operates without a catholyte, the main electrolyte effects involved here are primarily due to pH, cations, and anions caused by the ion-exchange membrane and the anode electrolyte.

pH Effect

The pH of the electrolyzer includes the local pH at the catalyst surface and the bulk pH in the solution. Because the CO_2RR is a proton-consuming multistep reaction, its process will cause a high local concentration of OH^- at the electrode–electrolyte interface, which could affect the dynamic equilibria among HCO_3^-, CO_2, and CO_3^{2-} during the CO_2RR [48, 49]. In addition, because of the competition with HER, the pH at the reaction interface has an important effect on the activity and selectivity of the CO_2RR [50–52]. Numerous excellent works have recently reported the influence of pH value in H-cells [53–57]. Although the pH differs between these two configurations during CO_2RR, commonalities are numerous. Here, we mainly discuss the research progress on the effect of pH on the CO_2RR in an MEA.

The transport of reactants and products in flow architectures through a flow field and GDE results in a high current density (≥ 100 mA/cm^2). Mass transfer and high current density affect the pH gradient near the catalyst surface in flow cells [58]. Zhang et al. [59] applied operando Raman spectroscopy to monitor the pH near the Ag catalyst surface profiles. The functions of pH and electrolytic time, operating current density,

distance from the catalyst surface, and temperature were investigated. They found that increasing the current density and temperature increases the surface pH and inhibits the HER (Fig. 6a–c). The temperature effect varies among MEA systems. She and coworkers [60] designed an AEM/proton-exchange membrane (PEM) assembly MEA system with pure H_2O as the anolyte to suppress/prevent carbonate formation/precipitation. They found that excessive reaction temperatures (e.g., 80 °C) suppressed the CO_2RR and made the HER dominant [60]. In addition, an anion exchange ionomer (AEI) layer was employed to enhance the localized pH within the MEA system by modulating the microenvironment surrounding the catalyst surface [61, 62]. Park et al. [63] examined the notable impact of AEI on local pH by in situ pH measurements in a CEM-based MEA system to improve the selectivity of the CO_2RR. They found that the local pH markedly increased from 5.338 to 9.628 as the AEI ratio increased from 5 wt% to 50 wt%, and the selectivity of CO increased from 9.8% to 60.4% (Fig. 6d–f). Furthermore, the authors show that high cation concentrations and thick carbon-containing CLs enhanced the neutralizing pH gradient and reduced the neutralizing boundary layer, which helps create an alkaline environment with high CO_2RR selectivity.
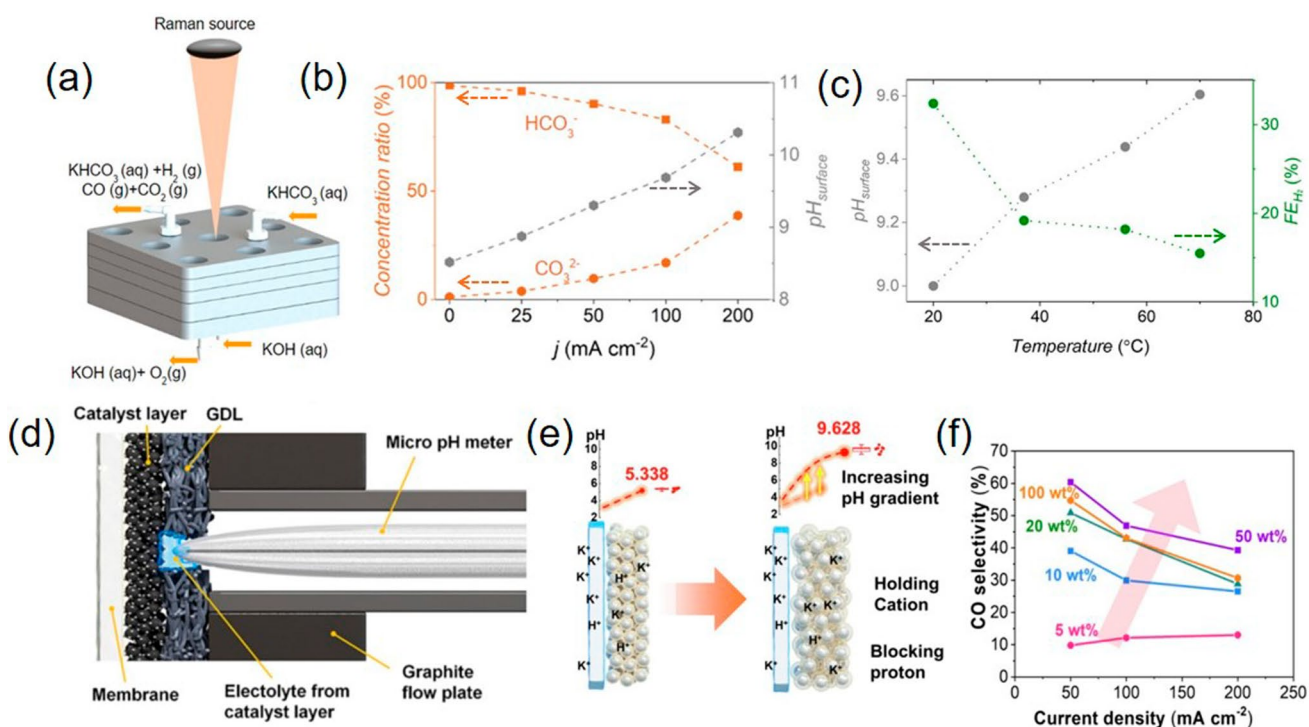

Fig. 6 a Assembled zero-gap bicarbonate flow cell for operando Raman spectroscopy. **b** Ratios of $[HCO_3^-]/[C_{total}]$ and $[CO_3^{2-}]/[C_{total}]$ and the corresponding calculated pH near the catalyst surface. **c** Impact of temperature on the surface pH and H_2 production. Reproduced with permission from Ref. [59]. Copyright 2020, American Chemical Society. **d** Schematics depicting the in situ measurement of pH in an MEA electrolyzer. **e** Schematic of the impact of AEI on pH. **f** Selective CO conversion at different AEI contents. Reproduced with permission from Ref. [63]. Copyright 2023, Elsevier

The local pH greatly influences the solubility of CO_2, the thermodynamics of the CO_2RR by the equilibrium reaction between $CO_2/CO_3^{2-}/HCO_3^-$ and the rate-limiting step of reactions; further investigation is needed in future CO_2RR MEA studies to determine the exact influence of pH.

Cation Effects

Several studies have indicated that alkali metal cations alter the selectivity and activity of CO_2RR products [64–66]. Using a copper electrode in hydrogen-carbonate solutions containing different specific cations, Hori et al. [67] conducted early research on the electroreduction of CO_2 and CO. They discovered that the presence of cations in the electrolyte considerably influences the distribution of products. They revealed that Li^+ has favorable H_2 evolution, while the Na^+ and Cs^+ share high FE for methane and C_2H_4, respectively. This difference in selectivity is related to the potential of the outer Helmholtz plane formed by different sizes of hydrated ions, which affects the concentration of H^+ on the electrode surface.

In the MEA electrolyzers, the cation in the anolyte can also reach the cathode surface through the ionic exchange membrane, which considerably impacts CO_2RR performance. Using $KHCO_3$ and $CsHCO_3$ electrolytes in a CEM-based MEA electrolyzer, Park et al. [63] investigated the effects of cations on the performance of Ag/C electrodes. They observed that the CO selectivity of Ag-Cs/C electrodes was higher than that of Ag-K/C electrodes, which

offers further evidence that larger cations encourage the CO_2RR. Furthermore, because of the strong barrier to Cs production at the CEM, the Ag-Cs/C electrode has a much higher cell voltage than the Ag-K/C electrode, which affects energy efficiency.

Compared to CEM-based MEA electrolyzers, the specific behavior of cations in AEM electrolyzers has received less attention. An ideal AEM should exhibit anion permeability while maintaining cation impermeability. However, in the case of K^+, cations can be transported from the anolyte to the cathode through the AEM, reacting with CO_3^{2-} produced by CO_2 passing through the alkaline GDE, resulting in solid carbonate precipitation (Fig. 7) [36]. The presence of these precipitates can lead to issues such as catalyst surface coverage, reduction in electrode hydrophobicity, and gas channel blockage, considerably impeding the long-term stability of the CO_2 electrolyzer. To alleviate this problem, pure water or an electrolyte containing Cs^+ can be used. Janaky et al. [68] proposed a method for enhancing the performance and durability of an AEM-based MEA electrolyzer operating with pure water. Their strategy involves deliberately introducing a small quantity of alkali metal cations (specifically Cs^+ and K^+) to the cathode. This infusion of cations activates and rejuvenates the electrolyzer, improving efficiency and stability. Additionally, it helps prevent degradation caused by carbonate precipitation.
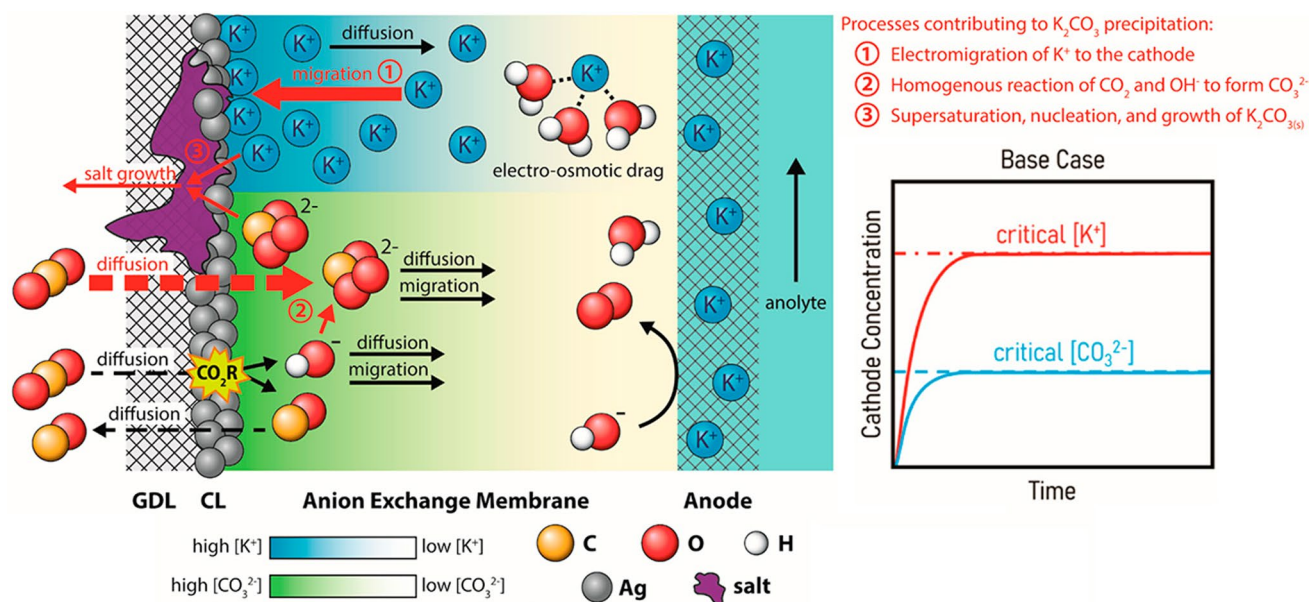

Fig. 7 Schematic representation of the cascade of reactions and ion transport in an AEM-based MEA leading to salt formation on the cathode. The inserted graph shows the change in ion concentrations occurring near the cathode. After both CO_3^{2-} and K^+ concentrations reach critical levels, the precipitation of K_2CO_3 starts to occur. Reproduced with permission from Ref. [36]. Copyright 2022, American Chemical Society

Anion Effects

Aside from cations, many experiments have proved that anions can influence the activity and selectivity of CO_2 reduction in catholyte-involved systems [57, 69, 70]. The anions in AEM-based MEA electrolyzers primarily originate from the anolyte, namely OH^- ions, as well as CO_3^{2-} and HCO_3^- generated through reactions involving OH^- and CO_2. HCO_3^- and CO_3^{2-} are commonly used electrolytes because they provide a near-neutral pH [71]. However, they are not the optimal option. The larger hydration radii and masses of CO_3^{2-} and HCO_3^- compared to OH^- result in considerably lower intrinsic mobility, leading to a 4–fivefold decrease in the ion conductivity of AEMs, which substantially increases cell resistance and lowers CO_2 utilization efficiency. OH^- can effectively inhibit the HER. Furthermore, an OH^--containing solution, such as aqueous KOH, has better electrical conductivity than $KHCO_3$, which can lower the Ohmic loss. However, an extremely alkaline environment harms the selectivity of the product [72]. Therefore, designing high carbonate ion conductance AEMs is a promising way to overcome the above competition.

Halide anions promote the activity of CO_2 reduction and are commonly used to study the effects of anions. The study conducted by Salazar-Villalpando et al. [73] revealed that halides in a solution enhance the reduction current of CO_2 on copper. This enhancement is due to the covalent interaction between Cu and halide, which facilitates the charge transfer between CO_2/CO and the Cu electrode. Lv and coworkers [74] modified the Cu surface with I^- from the electrolyte to facilitate C–C coupling on Cu-based catalysts toward multicarbon products in a neutral PEM electrolyzer, further demonstrating the importance of anions for the product selectivity of the CO_2RR. In addition, Strasser and colleagues [75] believed that the concentration and type of halide ion are key factors in adjusting the CO_2 reduction performance. They discovered that adding Cl^- and Br^- increases CO selectivity, while I^- was more conducive to methane formation. The surface's negative charge was enhanced in the following order: $Cl^- < Br^- < I^-$, due to the increased adsorption of halides. When I^- is adsorbed, the negative charge is transferred from I^- to the Cu surfaces, enhancing the CO protonation reaction. Wu et al. [76] enriched anions near the electrode by periodically applying a positive potential to the cathode. By adjusting the composition of KF, KCl, and $KHCO_3$ electrolytes, the ratio of C_1 and C_{2+} products can be precisely adjusted.

Because of the absence of a catholyte in MEAs and the predominant use of an alkaline electrolyte in the anolyte, research on the impact of halide ions from the anode electrolyte on MEA electrolyzer performance has been limited. Huang et al. [77] constructed a charged imidazolium functionalized porphyrin-based covalent organic framework (Co-iBFBim-COF-X) and investigated its electrocatalytic CO_2RR activity in an MEA. They found that the free anions can stabilize the key intermediate *COOH that favors the CO_2RR. In addition, the free halogen ions in the system hinder the HER by reducing the binding energy between H_2O and Co-porphyrin. Moreover, this study indirectly demonstrated the influence of free halide ions on the catalytic activity and selectivity of the CO_2RR in MEAs.

Anodic Reactions Paired with CO₂ Reduction

In the conventional CO_2 electrolysis process, the CO_2RR at the cathode necessitates an accompanying oxidation reaction at the anode. The oxygen evolution reaction (OER) has been extensively studied and comprehended, and substantial expertise has been accumulated in its catalysts, carriers, and other aspects. Therefore, the OER is selected as the initial paired anodic reaction for the CO_2RR. Recently, many MEA cells with the OER as the anode reaction have been designed to enhance the performance of the cathode CO_2RR [36, 38, 78]. However, the thermodynamic equilibrium potential of the OER (1.23 V vs. RHE) exceeds that of CO_2 reduction, leading to sluggish reaction kinetics and voltage and energy losses in the cell. Moreover, OER products (i.e., O_2) have less economic value than other chemical compounds, resulting in energy wastage during the transportation of O_2 [79, 80].

Based on the above considerations, the selection of organic (e.g., glycerol, methanol, and urea) anodic reactions with lower energy requirements than the OER and simultaneously yielding high-value chemicals will effectively reduce the overall energy consumption of the CO_2RR electrolytic system, thereby enhancing their economic feasibility (Fig. 8a) [81–84]. The methanol oxidation reaction (MOR) serves as a representative example of the overall coupling of CO_2 electrolysis. Zhou et al. [85] reported a partially pyrolyzed Ni-MOF electrocatalyst for an efficient MOR by in situ transformation of the Ni-OOH active phase. Applying this electrocatalyst to CO_2 electrolysis in an MEA system, the CO_2RR-MOR couple demonstrated exceptional performance for the electrosynthesis of formate and CO, with a high current density of ~ 500 mA/cm^2 at 2.2 V (Fig. 8b, c). Xie et al. [86] employed the glucose oxidation reaction to substitute for the OER at the anode of the CO_2RR MEA system, and by implementing a liquid–liquid anode process, they successfully circumvented the elevated energy loss associated with CO_2 recovery caused by O_2 mixing in conventional devices. The full-cell operates at a reduced voltage of 1.9 V while achieving an impressive overall carbon efficiency of 48%, thereby demonstrating a remarkable 46% reduction in energy
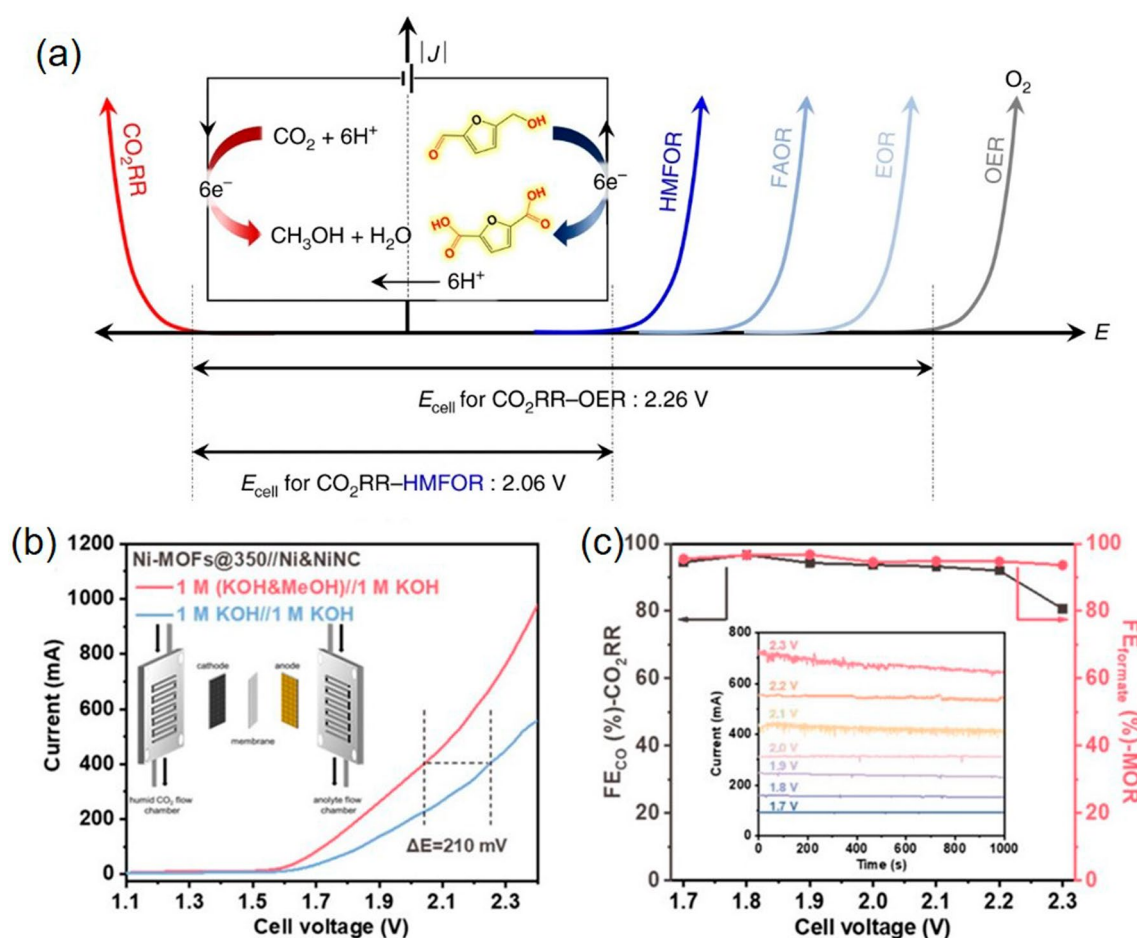
Fig. 8 a *I–V* curves and required potentials at the cathode and anode for electrolysis. Reproduced with permission from Ref. [81]. Copyright 2019, Nature Publishing Group. **b** Polarization curves and **c** voltage-dependent selectivity of Ni-MOF@350//Ni&NiNC in the MEA reactor. Reproduced with permission from Ref. [85]. Copyright 2023, American Chemical Society

intensity compared to currently available state-of-the-art single-stage CO_2 reduction devices.

In summary, the integration of CO_2 cathode reduction with the anodic oxidation of organic molecules through coelectrolysis in MEA cells exhibits the potential for reducing overall energy consumption and generating valuable organic products. However, studies in this area have been limited by the intricate nature of constructing a practical system (potential, product viability, market demand, and technical feasibility). Therefore, an anode system that complements the CO_2RR must be developed to enhance the economic viability of MEA electrolyzers.

Perspectives and Challenges

The conversion of CO_2 to high-value-added compounds by CO_2RR is an economically and technically feasible technology. This review primarily discusses the progress of MEA. The selection of key configurations that improve the overall performance of the CO_2RR is discussed. To date, great progress has been made in the realization of efficient electrochemical reduction of CO_2. However, the gap between the current technical level and the commercial production of the CO_2RR remains large. Several key challenges in the area need to be further addressed:

1. To meet future commercial production needs, the satisfactory stability of the system must be maintained. Thus far, the MEA has achieved a maximum recorded current density of 1 A/cm², well above the industry standard

(200 mA/cm^2), but can only operate for a few hundred hours, far less than 8000 h. The precise design of the GDE structure, the development of electrode treatment technology, and the reasonable selection of membrane materials are crucial for improving MEA stability.

2. The reduction of operational costs in the CO$_2$RR and the enhancement of the energy conversion efficiency are crucial factors for promoting advancements in this field. At present, the energy conversion efficiency of MEAs is seldom studied. With the development of this field and the technical maturity, it is necessary to reduce the electrolytic potential of the entire system and improve the conversion energy efficiency of the reaction. High value-added anodic oxidation products can be obtained by finding anodic reactions that can replace the OER, which not only helps improve the comprehensive utilization efficiency of electrical energy but also reduces the comprehensive cost of CO$_2$ electrochemical reduction.

3. The effect of gas purity on CO$_2$RR performance is crucial. To date, most studies on the CO$_2$RR have used high-purity CO$_2$ gas (> 99.999%) as a reactant, and the effect of gas impurities is largely unknown. Future CO$_2$ electrolysis processes will mostly use combustion waste gases from chemical and power plants as well as air that has been directly caught and is invariably contaminated with SO$_x$, NO$_x$, and a few volatile chemicals. How to enrich CO$_2$ gas, improve CO$_2$ concentration, and integrate it with MEAs has considerable research importance for realizing efficient and stable CO$_2$ reduction and transformation.

4. The reaction mechanism must be explored using characterization methods. The reaction mechanism in the microchannel electrochemical reactor is only observed from a macroscopic perspective; therefore, the study of its internal microscopic mechanism needs to be further explored, and the quantitative relationship between mass transfer and the reaction needs to be further studied. In situ characterization is crucial for comprehending CO$_2$RR behavior in an MEA configuration, but most existing in situ characterization methods only apply to observing the CO$_2$RR in H-cells. At present, in situ infrared and Raman spectroscopy, X-ray tomography, and laser scanning confocal microscopy in custom electrolytic cells provide new methods for studying the CO$_2$RR in MEA.

Declarations

Conflict of interest The authors declare that there is no conflict of interest.

References

1. Costentin C, Robert M, Savéant JM (2013) Catalysis of the electrochemical reduction of carbon dioxide. Chem Soc Rev 42(6):2423–2436
2. Schreier M, Héroguel F, Steier L et al (2017) Solar conversion of CO$_2$–CO using earth-abundant electrocatalysts prepared by atomic layer modification of CuO. Nat Energy 2(7):17087
3. Bushuyev OS, De Luna P, Dinh CT et al (2018) What should we make with CO$_2$ and how can we make it? Joule 2(5):825–832
4. Gao D, Wei P, Li H et al (2020) Designing electrolyzers for electrocatalytic CO$_2$ reduction. Acta Phys Chim Sin 37:2009020–2009021
5. Voiry D, Shin HS, Loh KP et al (2018) Low-dimensional catalysts for hydrogen evolution and CO$_2$ reduction. Nat Rev Chem 2:105
6. Lees EW, Mowbray BAW, Parlane FGL et al (2022) Gas diffusion electrodes and membranes for CO$_2$ reduction electrolysers. Nat Rev Mater 7:55–64
7. Zhang S, Fan Q, Xia R et al (2020) CO$_2$ reduction: from homogeneous to heterogeneous electrocatalysis. Acc Chem Res 53(1):255–264
8. Pan F, Yang Y (2020) Designing CO$_2$ reduction electrode materials by morphology and interface engineering. Energy Environ Sci 13(8):2275–2309
9. Gu J, Hsu CS, Bai L et al (2019) Atomically dispersed Fe^{3+} sites catalyze efficient CO$_2$ electroreduction to CO. Science 364(6445):1091–1094
10. Cheng Y, Hou P, Wang X et al (2022) CO$_2$ electrolysis system under industrially relevant conditions. Acc Chem Res 55(3):231–240
11. Lin R, Guo J, Li X et al (2020) Electrochemical reactors for CO$_2$ conversion. Catalysts 10(5):473
12. Overa S, Ko BH, Zhao Y et al (2022) Electrochemical approaches for CO$_2$ conversion to chemicals: a journey toward practical applications. Acc Chem Res 55(5):638–648
13. Rabiee H, Ge L, Zhang X et al (2021) Gas diffusion electrodes (GDEs) for electrochemical reduction of carbon dioxide, carbon monoxide, and dinitrogen to value-added products: a review. Energy Environ Sci 14(4):1959–2008
14. Wakerley D, Lamaison S, Wicks J et al (2022) Gas diffusion electrodes, reactor designs and key metrics of low-temperature CO$_2$ electrolysers. Nat Energy 7:130–143
15. Reyes A, Jansonius RP, Mowbray BAW et al (2020) Managing hydration at the cathode enables efficient CO$_2$ electrolysis at commercially relevant current densities. ACS Energy Lett 5(5):1612–1618
16. Ma D, Jin T, Xie K et al (2021) An overview of flow cell architecture design and optimization for electrochemical CO$_2$ reduction. J Mater Chem A 9(37):20897–20918
17. Weng LC, Bell AT, Weber AZ (2018) Modeling gas-diffusion electrodes for CO$_2$ reduction. Phys Chem Chem Phys 20(25):16973–16984
18. Lapicque F, Belhadj M, Bonnet C et al (2016) A critical review on gas diffusion micro and macroporous layers degradations for improved membrane fuel cell durability. J Power Sources 336:40–53

19. Leonard ME, Clarke LE, Forner-Cuenca A et al (2020) Investigating electrode flooding in a flowing electrolyte, gas-fed carbon dioxide electrolyzer. Chemsuschem 13(2):400–411

20. Shi R, Guo J, Zhang X et al (2020) Efficient wettability-controlled electroreduction of CO_2 to CO at Au/C interfaces. Nat Commun 11(1):3028

21. Gabardo CM, O'Brien CP, Edwards JP et al (2019) Continuous carbon dioxide electroreduction to concentrated multi-carbon products using a membrane electrode assembly. Joule 3(11):2777–2791

22. Velayutham G, Kaushik J, Rajalakshmi N et al (2007) Effect of PTFE content in gas diffusion media and microlayer on the performance of PEMFC tested under ambient pressure. Fuel Cells 7(4):314–318

23. Kim B, Hillman F, Ariyoshi M et al (2016) Effects of composition of the micro porous layer and the substrate on performance in the electrochemical reduction of CO_2 to CO. J Power Sources 312:192–198

24. Zhong M, Tran K, Min Y et al (2020) Accelerated discovery of CO_2 electrocatalysts using active machine learning. Nature 581(7807):178–183

25. Orogbemi OM, Ingham DB, Ismail MS et al (2016) The effects of the composition of microporous layers on the permeability of gas diffusion layers used in polymer electrolyte fuel cells. Int J Hydrog Energy 41(46):21345–21351

26. Wang Z, Li Y, Zhao X et al (2023) Localized alkaline environment via in situ electrostatic confinement for enhanced CO_2-to-ethylene conversion in neutral medium. J Am Chem Soc 145(11):6339–6348

27. Liu M, Hu H, Kong Y et al (2023) The role of ionomers in the electrolyte management of zero-gap MEA-based CO_2 electrolysers: a Fumion versus Nafion comparison. Appl Catal B Environ 335:122885

28. Merino-Garcia I, Alvarez-Guerra E, Albo J et al (2016) Electrochemical membrane reactors for the utilisation of carbon dioxide. Chem Eng J 305:104–120

29. Weekes DM, Salvatore DA, Reyes A et al (2018) Electrolytic CO_2 reduction in a flow cell. Acc Chem Res 51(4):910–918

30. Salvatore DA, Gabardo CM, Reyes A et al (2021) Designing anion exchange membranes for CO_2 electrolysers. Nat Energy 6:339–348

31. Kibria MG, Edwards JP, Gabardo CM et al (2019) Electrochemical CO_2 reduction into chemical feedstocks: from mechanistic electrocatalysis models to system design. Adv Mater 31(31):e1807166

32. Zheng Y, Jiao Y, Vasileff A et al (2018) The hydrogen evolution reaction in alkaline solution: from theory, single crystal models, to practical electrocatalysts. Angew Chem Int Ed Engl 57(26):7568–7579

33. Jiang K, Siahrostami S, Zheng T et al (2018) Isolated Ni single atoms in graphene nanosheets for high-performance CO_2 reduction. Energy Environ Sci 11(4):893–903

34. Yanagi R, Zhao T, Cheng M et al (2023) Photocatalytic CO_2 reduction with dissolved carbonates and near-zero CO_2(aq) by employing long-range proton transport. J Am Chem Soc 145(28):15381–15392

35. Hori Y, Ito H, Okano K et al (2003) Silver-coated ion exchange membrane electrode applied to electrochemical reduction of carbon dioxide. Electrochim Acta 48(18):2651–2657

36. Sassenburg M, Kelly M, Subramanian S et al (2022) Zero-gap electrochemical CO_2 reduction cells: challenges and operational strategies for prevention of salt precipitation. ACS Energy Lett 8(1):321–331

37. Xu Y, Miao RK, Edwards JP et al (2022) A microchanneled solid electrolyte for carbon-efficient CO_2 electrolysis. Joule 6(6):1333–1343

38. Pan B, Fan J, Zhang J et al (2022) Close to 90% single-pass conversion efficiency for CO_2 electroreduction in an acid-fed membrane electrode assembly. ACS Energy Lett 7(12):4224–4231

39. Lee W, Kim YE, Youn MH et al (2018) Catholyte-free electrocatalytic CO_2 reduction to formate. Angew Chem Int Ed Engl 57(23):6883–6887

40. Zhang Z, Huang X, Chen Z et al (2023) Membrane electrode assembly for electrocatalytic CO_2 reduction: principle and application. Angew Chem Int Ed Engl 62(28):e202302789

41. Xie K, Miao RK, Ozden A et al (2022) Bipolar membrane electrolyzers enable high single-pass CO_2 electroreduction to multicarbon products. Nat Commun 13(1):3609

42. Blommaert MA, Aili D, Tufa RA et al (2021) Insights and challenges for applying bipolar membranes in advanced electrochemical energy systems. ACS Energy Lett 6(7):2539–2548

43. McDonald MB, Ardo S, Lewis NS et al (2014) Use of bipolar membranes for maintaining steady-state pH gradients in membrane-supported, solar-driven water splitting. Chemsuschem 7(11):3021–3027

44. Vargas-Barbosa NM, Geise GM, Hickner MA et al (2014) Assessing the utility of bipolar membranes for use in photoelectrochemical water-splitting cells. Chemsuschem 7(11):3017–3020

45. Li YC, Zhou D, Yan Z et al (2016) Electrolysis of CO_2 to syngas in bipolar membrane-based electrochemical cells. ACS Energy Lett 1:1149–1153

46. Yang K, Li M, Subramanian S et al (2021) Cation-driven increases of CO_2 utilization in a bipolar membrane electrode assembly for CO_2 electrolysis. ACS Energy Lett 6(12):4291–4298

47. Vermaas DA, Smith WA (2016) Synergistic electrochemical CO_2 reduction and water oxidation with a bipolar membrane. ACS Energy Lett 1(6):1143–1148

48. Nitopi S, Bertheussen E, Scott SB et al (2019) Progress and perspectives of electrochemical CO_2 reduction on copper in aqueous electrolyte. Chem Rev 119(12):7610–7672

49. Zhong H, Fujii K, Nakano Y et al (2015) Effect of CO_2 bubbling into aqueous solutions used for electrochemical reduction of CO_2 for energy conversion and storage. J Phys Chem C 119(1):55–61

50. Ma M, Clark EL, Therkildsen KT et al (2020) Insights into the carbon balance for CO_2 electroreduction on Cu using gas diffusion electrode reactor designs. Energy Environ Sci 13(3):977–985

51. Liu M, Pang Y, Zhang B et al (2016) Enhanced electrocatalytic CO_2 reduction via field-induced reagent concentration. Nature 537(7620):382–386

52. Bohra D, Chaudhry JH, Burdyny T et al (2019) Modeling the electrical double layer to understand the reaction environment in a CO_2 electrocatalytic system. Energy Environ Sci 12(11):3380–3389

53. Li Z, Sun B, Xiao D et al (2023) Electron-rich Bi nanosheets promote $CO_2^{\cdot-}$ formation for high-performance and pH-universal electrocatalytic CO_2 reduction. Angew Chem Int Ed Engl 62(11):e202217569

54. Ma M, Djanashvili K, Smith WA (2016) Controllable hydrocarbon formation from the electrochemical reduction of CO_2 over Cu nanowire arrays. Angew Chem Int Ed Engl 55(23):6680–6684

55. Varela AS, Kroschel M, Leonard ND et al (2018) pH effects on the selectivity of the electrocatalytic CO_2 reduction on graphene-embedded Fe–N–C motifs: bridging concepts between molecular homogeneous and solid-state heterogeneous catalysis. ACS Energy Lett 3(4):812–817

56. Baricuatro JH, Kwon S, Kim YG et al (2021) Operando electrochemical spectroscopy for CO on Cu(100) at pH 1–13:validation of grand canonical potential predictions. ACS Catal 11(5):3173–3181

57. Sebastián-Pascual P, Petersen AS, Bagger A et al (2021) pH and anion effects on Cu–phosphate interfaces for CO electroreduction. ACS Catal 11(3):1128–1135

58. Lu X, Zhu C, Wu Z et al (2020) In situ observation of the pH gradient near the gas diffusion electrode of CO₂ reduction in alkaline electrolyte. J Am Chem Soc 142(36):15438–15444

59. Zhang Z, Melo L, Jansonius RP et al (2020) pH matters when reducing CO₂ in an electrochemical flow cell. ACS Energy Lett 5(10):3101–3107

60. She X, Zhai L, Wang Y et al (2024) Pure-water-fed, electrocatalytic CO₂ reduction to ethylene beyond 1000 h stability at 10 A. Nat Energy 9:81–91

61. O'Brien CP, Miao RK, Liu S et al (2021) Single pass CO₂ conversion exceeding 85% in the electrosynthesis of multicarbon products via local CO₂ regeneration. ACS Energy Lett 6(8):2952–2959

62. Kim C, Bui JC, Luo X et al (2021) Tailored catalyst microenvironments for CO₂ electroreduction to multicarbon products on copper using bilayer ionomer coatings. Nat Energy 6:1026–1034

63. Park J, Ko YJ, Lim C et al (2023) Strategies for CO₂ electroreduction in cation exchange membrane electrode assembly. Chem Eng J 453:139826

64. Le D, Rahman TS (2022) On the role of metal cations in CO₂ electrocatalytic reduction. Nat Catal 5:977–978

65. Bhugun I, Lexa D, Savéant JM (1996) Catalysis of the electrochemical reduction of carbon dioxide by iron (0) porphyrins synergistic effect of Lewis acid cations. J Phys Chem 100(51):19981–19985

66. Jin Z, Guo Y, Qiu C (2022) Electro-conversion of carbon dioxide to valuable chemicals in a membrane electrode assembly. Sustainability 14(9):5579

67. Murata A, Hori Y (1991) Product selectivity affected by cationic species in electrochemical reduction of CO₂ and CO at a Cu electrode. Bull Chem Soc Jpn 64(1):123–127

68. Endrődi B, Samu A, Kecsenovity E et al (2021) Operando cathode activation with alkali metal cations for high current density operation of water-fed zero-gap carbon dioxide electrolyzers. Nat Energy 6(4):439–448

69. Hsieh YC, Senanayake SD, Zhang Y et al (2015) Effect of chloride anions on the synthesis and enhanced catalytic activity of silver nanocoral electrodes for CO₂ electroreduction. ACS Catal 5(9):5349–5356

70. Resasco J, Lum Y, Clark E et al (2018) Effects of anion identity and concentration on electrochemical reduction of CO₂. ChemElectroChem 5(7):1064–1072

71. Deng B, Huang M, Zhao X et al (2021) Interfacial electrolyte effects on electrocatalytic CO₂ reduction. ACS Catal 12(1):331–362

72. Gabardo CM, Seifitokaldani A, Edwards JP et al (2018) Combined high alkalinity and pressurization enable efficient CO₂ electroreduction to CO. Energy Environ Sci 11(9):2531–2539

73. Ogura K, Ferrell JR, Cugini AV et al (2010) CO₂ attraction by specifically adsorbed anions and subsequent accelerated electrochemical reduction. Electrochim Acta 56(1):381–386

74. Lv X, Yang Y, Lv J et al (2023) Iodine-mediated C—C coupling in neutral flow cell for electrochemical CO₂ reduction. Adv Funct Mater 34:2311236

75. Varela AS, Ju W, Reier T et al (2016) Tuning the catalytic activity and selectivity of Cu for CO₂ electroreduction in the presence of halides. ACS Catal 6(4):2136–2144

76. Wang J, Qin Y, Jin S et al (2023) Customizing CO₂ electroreduction by pulse-induced anion enrichment. J Am Chem Soc 145(48):26213–26221

77. Wu QJ, Si DH, Wu Q et al (2023) Boosting electroreduction of CO₂ over cationic covalent organic frameworks: hydrogen bonding effects of halogen ions. Angew Chem Int Ed Engl 62(7):e202215687

78. Yun H, Choi W, Shin D et al (2023) Atomic arrangement of AuAg alloy on carbon support enhances electrochemical CO₂ reduction in membrane electrode assembly. ACS Catal 13(13):9302–9312

79. Li D, Yang J, Lian J et al (2023) Recent advances in paired electrolysis coupling CO₂ reduction with alternative oxidation reactions. J Energy Chem 77:406–419

80. Chen H, Ding C, Kang C et al (2023) The design of alternative anodic reactions paired with electrochemical CO₂ reduction. Green Chem 25(14):5320–5337

81. Na J, Seo B, Kim J et al (2019) General technoeconomic analysis for electrochemical coproduction coupling carbon dioxide reduction with organic oxidation. Nat Commun 10(1):5193

82. Verma S, Lu S, Kenis PJA (2019) Co-electrolysis of CO₂ and glycerol as a pathway to carbon chemicals with improved technoeconomics due to low electricity consumption. Nat Energy 4:466–474

83. Wei X, Li Y, Chen L et al (2021) Formic acid electro-synthesis by concurrent cathodic CO₂ reduction and anodic CH₃OH oxidation. Angew Chem Int Ed Engl 60(6):3148–3155

84. Cao C, Ma DD, Jia J et al (2021) Divergent paths, same goal: a pair-electrosynthesis tactic for cost-efficient and exclusive formate production by metal-organic-framework-derived 2D electrocatalysts. Adv Mater 33(25):e2008631

85. Zhou Y, Wang Z, Fang W et al (2023) Modulating O–H activation of methanol oxidation on nickel-organic frameworks for overall CO₂ electrolysis. ACS Catal 13(3):2039–2046

86. Xie K, Ozden A, Miao RK et al (2022) Eliminating the need for anodic gas separation in CO₂ electroreduction systems via liquid-to-liquid anodic upgrading. Nat Commun 13:3070

Yuhui Chen obtained his Bachelor's degree in Fudan University in 2009, and received his Ph.D. degree from University of St Andrews (United Kingdom) in 2014. Later, he worked with Prof. Peter Bruce at the University of Oxford (United Kingdom) on the topic of metal–air batteries. Since 2017, he is the professor at Nanjing Tech University. His research interests include in situ electrochemistry techniques, reaction mechanisms for Li-air batteries, and CO₂ electrochemical catalysis.